이학석사 학위논문

The role of arachidonic acid 12-lipoxygenase (ALOX12) in pulmonary fibrosis

폐 섬유화에서 ALOX12의 역할

울 산 대 학 교 대 학 원

의 과 학 과

황 기 원

The role of arachidonic acid 12-lipoxygenase (ALOX12) in pulmonary fibrosis

지 도 교 수 송 진 우

이 논문을 이학석사 학위 논문으로 제출함

2022 년 2월

울 산 대 학 교 대 학 원
의 과 학 과
황 기 원

황기원의 이학석사 학위 논문을 인준함

심사위원 황 정 진 (인)

심사위원 홍 석 찬 (인)

심사위원 송 진 우 (인)

울 산 대 학 교 대 학 원

2022 년 2 월

Abstract

Background: 12(S)-hydroxyeicosatetraenoic acid (12(S)-HETE) is a product of arachidonic acid metabolism produce by arachidonic acid 12-lipoxygenase (ALOX12) in human platelets or leukocytes. It was well known that ALOX12 plays an important role in inflammation and oxidation and is involved in development of various human diseases. However, the role of 12(S)-HETE and ALOX12 in the pathogenesis of idiopathic pulmonary fibrosis (IPF) remains unexplored. Therefore, we investigated the role of ALOX12 in IPF in this study.

Methods: The level of 12(S)-HETE was measured in human plasma (healthy control = 40, IPF = 76) by liquid chromatography-mass spectrometry (LC-MS/MS). The function of 12(S)-HETE and ALOX12 were evaluated in transforming growth factor beta-1 (TGF-β1)-stimulated human lung fibroblasts (MRC-5 cell and primary lung fibroblast) using ALOX12 inhibitor or RNA interference (RNAi). The anti-fibrotic effect of ALOX12 inhibitor was assessed through cell migration assay and evaluated in pulmonary fibrosis mice model induced by bleomycin.

Results: The levels of 12(S)-HETE were significantly increased in plasma of IPF patients compared with that of controls. Exposure of human lung fibroblast to 12(S)-HETE increased the expression of collagen I and fibronectin in human lung fibroblast. In addition, the levels of ALOX12 were increased in lung tissues of patients with IPF and human lung fibroblasts stimulated by TGF-β1 compared with those of controls. ALOX12 inhibitor and ALOX12 specific siRNA downregulated protein expression of collagen I and fibronectin increased by TGF-β1 in human lung fibroblasts. ALOX12 inhibitor also suppressed migration and TGF-β1 induced phosphorylation of Smad2/3 in MRC-5 cells. In bleomycin treated mice,

administration of ALOX12 inhibitor decreased levels of hydroxyproline in the lung compared of control mice.

Conclusions: These results suggest that inhibition of ALOX12 may have anti-fibrotic effects on pulmonary fibrosis, suggesting that ALOX12 is implicated as a potential therapeutic target in IPF.

Keywords: 12(S)-HETE, ALOX12, idiopathic pulmonary fibrosis

Contents

Abbreviations

ALOX12: Arachidonic acid 12-lipoxygenase

12(S)-HETE: 12(S)-hydroxyeicosatetraenoic acid

12(S)-HPETE: 12(S)-hydroperoxyeicosatetraenoic acid

IPF: Idiopathic pulmonary fibrosis

TGF-β1: Transforming growth factor beta-1

AA: Arachidonic acid

LC-MS/MS: Liquid chromatography-mass spectrometry

siRNA: Small interfering RNA

PVDF: Polyvinylidene fluoride

BSA: Bovine serum albumin

ROC : Receiver operating characteristic

FVC: Forced vital capacity

DLco: Diffusing capacity of the lung for carbon monoxide

TLC: Total lung capacity

Introduction

Idiopathic pulmonary fibrosis (IPF) is a chronic progressive fibrosing interstitial lung disease of unknown etiology with a poor prognosis of median survival of 3 years [1, 2]. IPF is developed by an alveolar injury due to unidentified causes that leads to activation of fibroblasts [3]. Differentiation to myofibroblast induced by TGF-β1 is important in various fibrotic diseases including pulmonary fibrosis, liver cirrhosis, and renal fibrosis [4]. Also, aberrant wound healing responses to alveolar epithelial injury including abnormal fibroblast proliferation, and excessive accumulation of extracellular matrix proteins have been implicated in the pathogenesis of IPF [5-7]. Currently, two anti-fibrotic agents, nintedanib and pirfenidone, are known to slow progression of IPF [8, 9]; however, these drugs does not halt or reverse progression of pulmonary fibrosis. Lipids metabolites and dysregulation of lipid metabolism has been implicated to be important in the pathogenesis of IPF [10, 11]. Actually, some of the lipid metabolites and associated enzymes have been targeted for drug developments for IPF [10].

The arachidonic acid (AA) metabolism is known to have important roles in the development and progression of cardiovascular disease, obesity, diabetes, cancer, and inflammatory diseases [12-14]. AA is converted to eicosanoids by arachidonic acid lipoxygenase (ALOX) enzymes [15]. It is known that in human species, three isoforms (ALOX5, ALOX12 and ALOX15) are present. ALOX12 catalyzes peroxidation of arachidonic acid to 12S-hydroperoxyeicosatetraenoic acid (12(S)-HPETE), which is rapidly reduced to 12(S)-HETE [16-18]. ALOX12 and 12(S)-HETE can generate ROS by increasing the activity of NADPH oxidase in the pancreatic β cell [19]. The role of ALOX12 or its related metabolites

in human lung disease has been reported [20-24]. Previous study has suggested that ALOX12, the human 12/15-lipoxygenase orthologue, is expressed in cavitary lesions and is associated with the downregulation of surfactant protein D in the lungs of patients with tuberculosis. Also, it is known that ALOX12 expression is high in patients with pulmonary injury caused by sulfur mustard. Moreover, previous studies suggested the role of ALOX12 in the pathogenesis of pulmonary fibrosis. ALOX12 induces aging of type II pneumocytes (AECIIs) in a NADPH oxidase 4 (NOX4) dependent manner. In addition, 12(S)-HETE, ALOX12 downstream product, is known to increase the expression of anti-inflammatory cytokine such as IL-13, which plays an important role in diseases such as radiation-induced pulmonary fibrosis (RIPF). However, the role of ALOX12 is still not well defined in the pathogenesis of pulmonary fibrosis. Therefore, the aim of this study was to evaluate the role of ALOX12 in the pathogenesis of IPF using *in vitro* and *in vivo* pulmonary fibrosis models.

Materials and methods

1. Human subjects

All IPF patients met the diagnostic criteria of the American Thoracic Society/European Respiratory Society/Japanese Respiratory Society/Latin American Thoracic Association [25]. IPF lung tissues (n = 6) were obtained at the time of surgical lung biopsy, and control human lung tissues (n = 6; normal lung tissues of lung cancer patients) with no histological evidence of disease were obtained from the Bio-Resource Center of Asan Medical Center, Seoul Republic of Korea. Plasma (n = 76) was also obtained from patients with IPF and healthy control (n = 40) from the Bio-Resource Center of Chungnam Medical Center, Chungnam, Republic of Korea.

2. Ethics statement

Lung tissue and plasma procurement was completed under Protocol #2016-1366, which was approved by the Institutional Review Board of Asan Medical Center. Written informed consent was obtained from all study participants. Mouse experiments were performed in accordance with the Guiding Principles for the Care and Use of Animals, and protocols were approved by the Animal Care and Handling Committee of Asan Medical Center (protocol #2017-12-034). While conducting the experiments, care was taken to minimize animal suffering.

3. Measurement of eicosanoids by LC-MS/MS

Eicosanoids were extracted from 400~900 μL of human plasma using solid phase extraction (SPE) described in the previous report [26]. Briefly, 60 mg Oasis HLB (Waters) SPE cartridge was washed and preconditioned with ethyl acetate, methanol and 0.1 % acetic acid: 5 % methanol in H_2O, sequentially. 10 μL of 0.2 mg/mL of EDTA and BHT in MeOH: H_2O (50:50) were added to sorbent bed of a SPE column. CUDA (1-cyclohexyl-dodecanoic acid urea), AUDA (12-[[(tricyclo[3.3.1.13,7]dec-1-ylamino)carbonyl]amino]-dodecanoic acid), PGE_2-d_4, and 9(10) EpOME-d_4 ([±]-12[13)-epoxy-9Z-octadecenoic acid- d_4) were also added as internal standards into samples. Sample solution was added into SPE column. The column was washed with 2 column volumes of 0.1 % acetic acid: 5 % methanol in H_2O, then the column was dried using vacuum. Finally, eicosanoids were eluted with 0.5 mL methanol, followed by 1.5 mL ethyl acetate. Sample solutions were dried using vacuum centrifuge, then stored at -20 °C until analysis. The dried matter was reconstituted with 20 μL of 50 % ACN prior to LC-MS/MS analysis. Eicosanoids and other chemicals were purchased from Cayman chemicals (Ann Arbor, MI) or Sigma-Aldrich (St. Louis, MO).

A liquid chromatography-tandem mass spectrometry system equipped with 1290 HPLC (Agilent), Qtrap 5500 (ABSciex) and reverse phase column (Pursuit 5 C18 150 × 2.1 mm) was used. Mobile phase A was 0.1 % acetic acid in H_2O and mobile phase B was 0.1 % acetic acid in ACN/MeOH (84/16, v/v). Flow rate was 250 μL/min and column oven was set at 25°C. The separation gradient was as follows: 35 to 45 % of B for 1.25 min, 45 to 55 % of B for 2 min, 55 to 66 % of B for 5.5 min, 66 to 72 % of B for 4 min, 72 to 82 % of B for 2.5 min, 82 to 95 % of B for 1.5 min, hold at 95 % of B for 1.5 min, 95 to 35 % of B for 0.1 min, and then hold at 35 % of B for 3.9 min. The multiple reaction monitoring (MRM) mode was

used in negative ion mode, and the extracted ion chromatogram corresponding to the specific transition of each analyte was used for quantification. The calibration range for each analyte was 0.1−10000 nM ($r^2 \geq 0.99$). Data analysis was performed by using either Analyst 1.5.2.

4. Cell culture

MRC-5 cells, a normal human lung fibroblast, were purchased from the American Type Culture Collection (ATCC) (Manassas, Virginia, USA), and the primary human lung fibroblasts were isolated form lung tissues from patients with IPF. To isolate primary fibroblasts from IPF patients, lung tissues were cut into 1 x 1 mm^2 pieces, and maintained at 37 °C in 5 % CO_2 humidified incubator for 7-10 days. These cells were maintained in eagle's minimal essential medium (EMEM; ATCC, Manassas, Virginia, USA) supplemented with 10 % fetal bovine serum (FBS, HyClone, Logan, USA), 100 U/mL penicillin and 100 μg/mL streptomycin (Invitrogen, Carlsbad, CA, USA). To maximize the drug's effectiveness, media was replaced with 0.5 % FBS, and then cells were treated with 5 ng/mL of TGF-β1 for 24 hours in the presence or absence of ALOX12 inhibitor (ML355, Cayman chemicals, Ann Arbor, Michigan, USA).

5. Antibody

Antibodies against ALOX12 were purchased from Invitrogen (Carlsbad, CA, USA; Cat No. PA5-26020), and those against fibronectin (Cat No. ab2413), collagen I (Cat No. ab34710) and α-SMA (Cat No. ab5694) were from Abcam (Cambridge, UK). Moreover, antibodies against

α-actinin were purchased from Santa Cruz Biotechnology (Santa Cruz, CA, USA; Cat No. sc17829) and those against phospho-Smad2 (Cat No. #3108), phospho-Smad3 (Cat No. #9520), Smad2 (Cat No. #3122) and Smad3 (Cat No. #9513) from Cell Signaling Technology (Beverly, MA, USA). The dilution ratio of primary antibodies used in this experiment was unified to 1:1000

6 . Western blotting

Cells were harvested in Dulbecco's phosphate buffered saline (DPBS, Welgene, Daegu, Korea) and centrifuged at 13,000 rpm in 4 °C for 1 min. Cell pellets were lysed in RIPA buffer (50 mM Tris-HCl, pH 7.5, 1 % Triton X-100, 150 mM NaCl, 1 % sodium deoxycholate, 2 mM EDTA, and 0.1 % sodium dodecyl sulfate), proteinase inhibitor cocktail (Sigma-Aldrich, St. Louis, MO, USA) and phosphatase inhibitor cocktail (Sigma-Aldrich, St. Louis, MO, USA). Cell pellets were centrifuged for 13,000 rpm at 4 °C for 15 min to take supernatant. Total protein concentration was quantified with the pierce BCA protein assay kit (Thermo Fisher Scientific, MA, USA). Proteins were separated using 10 % SDS-polyacrylamide gel electrophoresis (PAGE) and transferred to polyvinylidene fluoride (PVDF) membranes at 300 mA, 4°C, for 1 hour. In the protein-transferred membrane, non-specific protein binding was blocked with 5 % bovine serum albumin (BSA) and TBST (0.1 % Tween 20 in Tris-buffered saline) buffer for 1 hour at room temperature. The primary antibodies was diluted with 5 % BSA in TBST solution and blots were incubated overnight at 4 °C. The next day, blots were washed at room temperature and were incubated with HRP-conjugated IgG secondary antibody purchased from Sigma-Aldrich (ST Louis, MO, USA). ECL substrates, Supersignal West Pico

(Thermo Fisher Scientific, MA, USA) were used as the HRP substrate. Immunoreactive bands were analyzed with an enhanced chemiluminescence detection system (Pierce Biotechnology, Inc. Rockford, USA) and quantification of protein bands was performed using Image J analysis software (NIH, Bethesda, USA).

7. Wound healing assay

MRC-5 cells were grown in 60 mm cell culture dishes and cultured to 100% confluence and serum starved for 24 hours. Cells were scratched with 200 μL pipette tip, and washed twice using DPBS after taking photos of 0 hour. And then vehicle (DMSO, Sigma-Aldrich (ST Louis, MO, USA); Cat No. D2650), ML355 (10 μM) and TGF-β1 (5 ng/ml) were added to cells and incubated for 24 hours. The migration images of 24 hour were analyzed using microscope (Olympus CKX53, Tokyo, Japan) and EPview software (Olympus Life Science, Tokyo, Japan). Four experiments were repeated and the cell migration distance was calculated as a fold ratio.

8. siRNA transfection

ALOX12 specific siRNA (h) (sc-45984) and control siRNA (sc-37007) were purchased from Santa Cruz Biotechnology (Santa Cruz, CA, USA). MRC-5 cells were transfected for 48 hours with 30 pmol of ALOX12 specific siRNA or control siRNA using Lipofectamine 3000 reagent (Thermo Fisher Scientific, MA, USA) according to the manufacturer's instructions. Cells were harvested and analyzed by Western blot.

9. Animal model

Six-week-old female C57BL/6 mice were obtained from Orient Bio (Seongnam, South Korea) and acclimatized for 1 weeks before the experiments. The mice were randomly divided into four groups and were administered; 1) saline plus vehicle, 2) saline plus ML355, 3) bleomycin (3 U/kg) plus vehicle, 4) bleomycin plus ML355. Saline or bleomycin was injected intratracheally, and ML355 was administered by oral gavage at a dose of 15 mg/kg every 2 days for 2 weeks from 7 days after bleomycin treatment. The mice were sacrificed, and their lungs were harvested on day 21. All samples were snap-frozen in liquid nitrogen and stored at -80 °C. The grade of fibrosis was scored using the average of microscopic field scores [27].

10. Hydroxyproline assay

The lung tissues were weighed, homogenized in sterile water, add 10 N concentrated NaOH to samples and hydrolyzed in 10 N HCl at 120 °C for 1 hours. Then, they were cooled to room temperature and centrifuged at 10,000 xg for 5 minutes. Collect supernatant and transfer to a new tube. 10 μL of supernatant was added to plate and incubated at 65 °C for 2 hours. After that, chloarmine T solution (chloaramine T and citrate/acetate buffer [5 % citric acid, 1.2 % glacial acetic acid, 7.24 % sodium acetate and 3.4 % sodium hydroxide]) was added to the plate and incubated at room temperature for 20 min. After that, the hydrolyzed samples were incubated at 60 °C for 20 min with the addition of 100 μL Enrlich's solution (4-[dimethylamino] benzaldehyde [DMAB], isopropanol and perchloric acid). After incubated at 65 °C for 30 minutes, the absorbance of oxidized hydroxyproline was read at 560 nm. The amount of hydroxyproline was expressed as hydroxyproline contents / lung tissue (μg/ lung tissue).

11. Statistical analysis

All data values are expressed as mean ± standard deviation. Experiments were performed at least triplicate. The Student's t-test or the Mann-Whitney U test was used for continuous variables. All *P*-values were two-tailed, and $P < 0.05$ was used to indicate statistical significance. All statistical analyses were performed using GraphPad Prism Version 5 (GraphPad Software, La Jolla, CA, USA).

Results

The level of 12(S)-HETE is elevated in plasma of patients with IPF

We measured eicosanoids in human plasma (control = 40, IPF patients = 76) by LC-MS/MS. IPF group had older age and more frequent male than control group (Table 1). We focused eicosanoids with altered levels in plasma of patients with IPF. Among them, 12(S)-HETE levels were significantly higher in IPF patients than those in controls (Fig. 1A). Receiver operating characteristic (ROC) curve analysis revealed that 12(S)-HETE was useful in discriminating IPF from control (AUC=0.990, p= 0.001; the optimal cut-off value= 2.822 fmol/μL) (Fig. 1B).

Table 1. Comparison of the baseline characteristics between IPF patients and controls

Characteristics	IPF	Control	*P*-value
Number	76	40	
Age, years	74.2 ± 8.5	58.1 ± 4.5	< 0.001
Male	56 (73.7)	15 (37.5)	< 0.001
Ever-smokers	52 (68.4)	N/A	N/A
FVC % predicted	65.6 ± 14.5	N/A	N/A
DL_{co} % predicted	51.0 ± 16.9	N/A	N/A
TLC % predicted	65.8 ± 15.9	N/A	N/A

Data are presented as mean ± standard deviation or number (%), unless otherwise indicated.

IPF, idiopathic pulmonary fibrosis; FVC, forced vital capacity; DLco, diffusing capacity of the lung for carbon monoxide; TLC, total lung capacity.

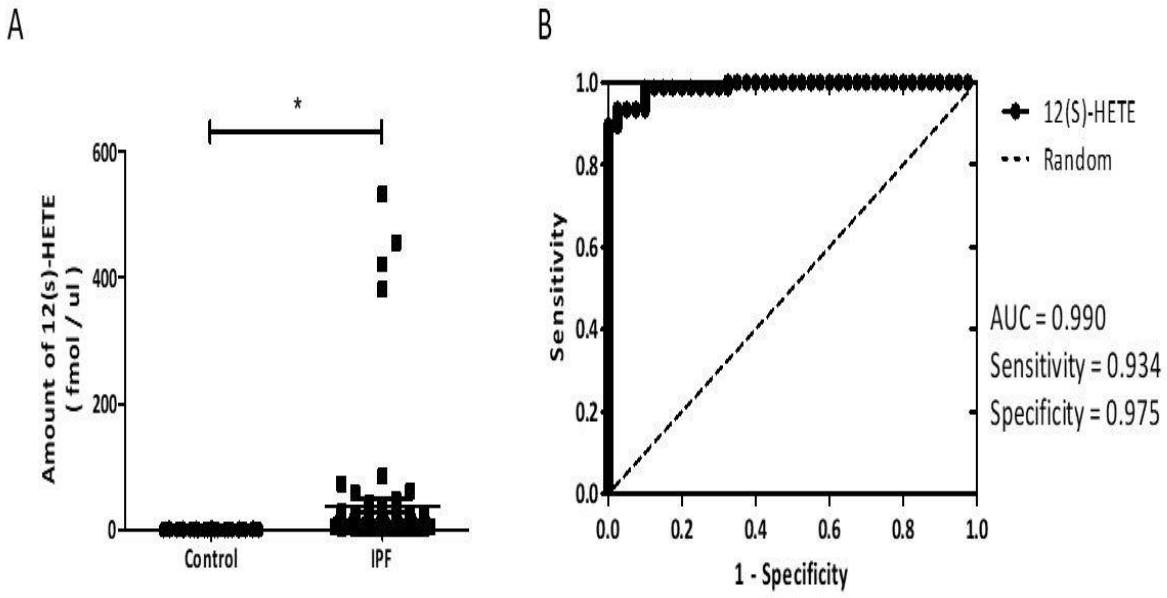

Figure 1. The plasma levels of 12(S)-HETE are elevated in IPF patients compared with controls

Quantification of eicosanoid metabolites in human plasma (control = 40, IPF patients = 76) by liquid chromatography with tandem mass spectrometry. (A) IPF patients showed higher levels of 12(S)-HETE than controls. (B) The ROC curve of 12(S)-HETE levels for diagnosis of IPF. * indicates $p < 0.001$ compared with controls; t- test.

12(S)-HETE potentiates pulmonary fibrosis in in vitro models

Based on the results of metabolomics for eicosanoids in human plasma, we investigated whether 12(S)-HETE involved in the pathogenesis of IPF. First, we examined the effects of 12(S)-HETE on the activation of fibroblast. In MRC-5 cell and primary human lung fibroblasts, treatment with 12(S)-HETE increased the levels of fibronectin and collagen I proteins in a dose-dependent manner (Fig. 2A-D).

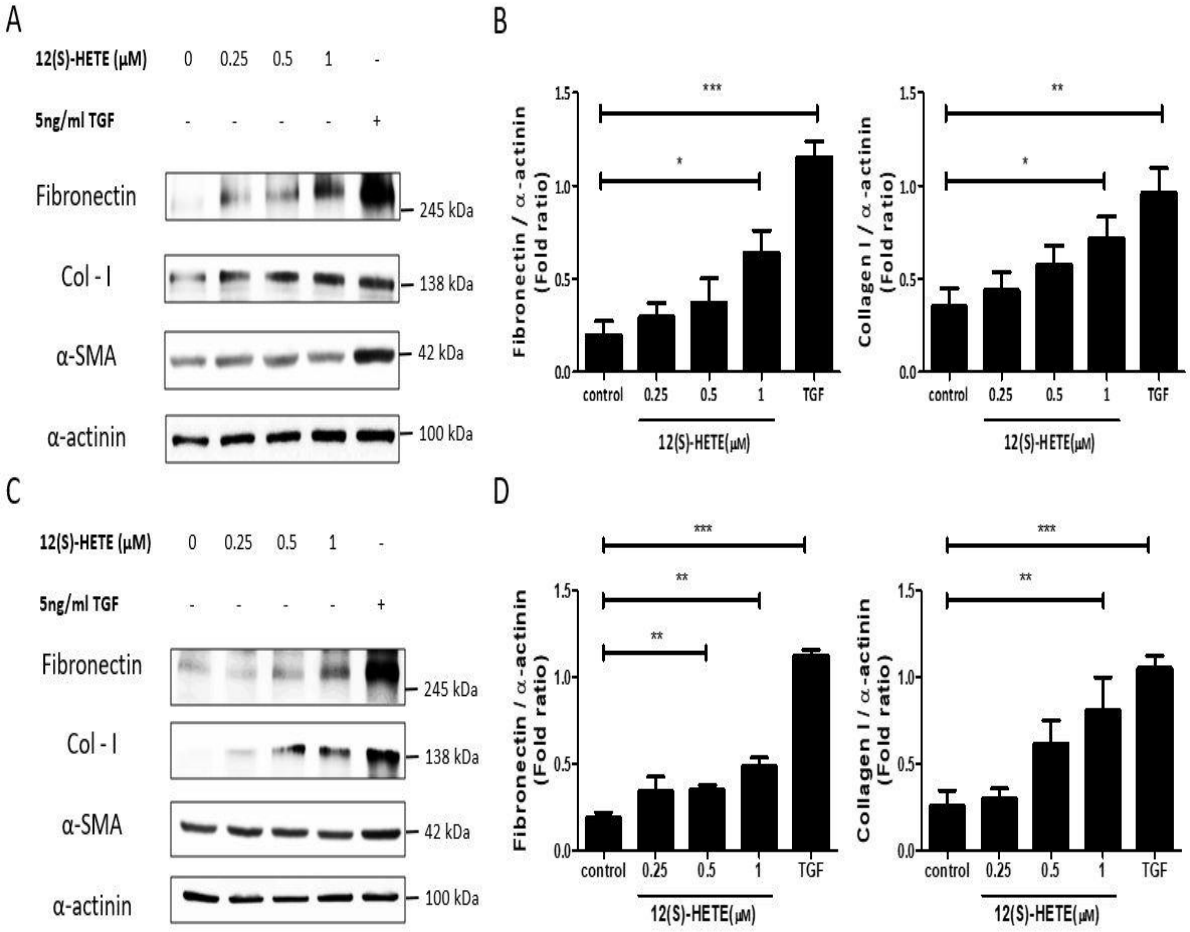

Figure 2. 12(S)-HETE shows pro-fibrotic effects in human lung fibroblasts

(A) MRC-5 cells were treated with 0.25, 0.5, and 1 μM of 12(S)-HETE for 24 hours. Then, fibronectin, collagen I, and α-SMA levels were measured by Western blot. (B) Densitometry was used to analyze fold changes in the levels of fibronectin/α-actinin and collagen I/α-actinin. * indicates $p < 0.05$, ** indicates $p < 0.01$ and *** indicates $p < 0.001$ compared with control. (C) Primary human lung fibroblasts were treated with 0.25, 0.5, and 1 μM of 12(S)-HETE for 24 hours. (D) Densitometry was used to analyze fold changes in the levels of fibronectin/α-actinin and collagen I/α-actinin. * indicates $p < 0.05$, ** indicates $p < 0.01$ and *** indicates $p < 0.001$ compared with control.

The expression of ALOX12 is elevated in the lung tissues of patients with IPF

Since 12(S)-HETE, arachidonic acid-derived metabolite, is catalyzed by ALOX12 [18], I confirmed the expression of ALOX12 in lung tissues of patients with IPF, based on the high expression of 12(S)-HETE in plasma of patients with IPF. I measured ALOX12 in human lung tissues (control = 6, IPF patients = 6) by Western blotting. The IPF group had a lower lung function than the control group (Table 2). I measured the protein levels of collagen I and ALOX12 in human lung tissues of IPF and control; the levels of ALOX12 and collagen I were significantly increased in patients with IPF (n=6) compared with controls (n=6) (Fig. 3A,B).

Table 2. Comparison of the baseline characteristics between IPF patients and controls

Characteristics	IPF	Control	*P*-value
Number	6	6	
Age, years	74.17 ± 15.5	69.82 ± 7.19	0.548
Male	4 (66.6)	5 (83.3)	0.549
Ever-smokers	3 (50.0)	5 (83.3)	0.259
FVC % predicted	71.8 ± 19.5	95.3 ± 13.4	0.035
DL_{co} % predicted	54.3 ± 20.6	96.17 ± 14.9	0.002
TLC % predicted	75.6 ± 10.6	101 ± 6.6	0.01

Data are presented as mean ± standard deviation or number (%), unless otherwise indicated.

IPF, idiopathic pulmonary fibrosis; FVC, forced vital capacity; DLco, diffusing capacity of the lung for carbon monoxide; TLC, total lung capacity.

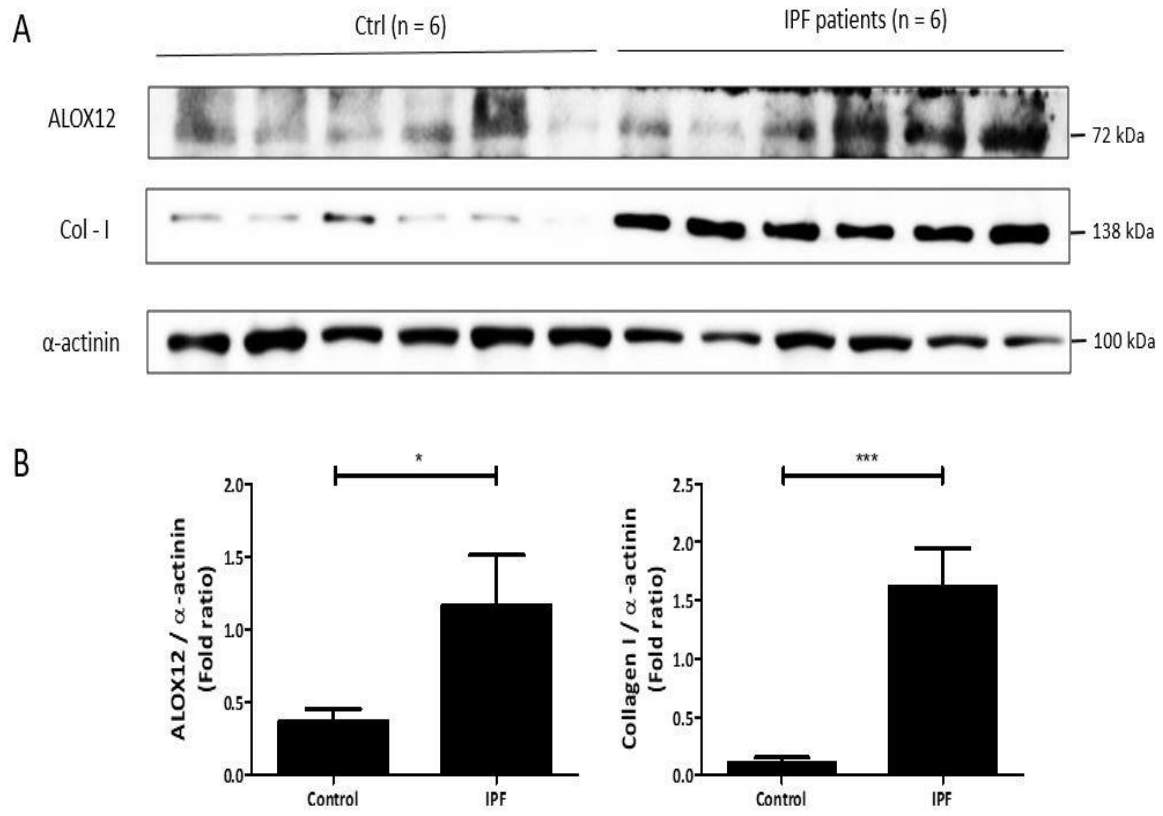

Figure 3. ALOX12 levels are increased in lung tissues of IPF patients

(A) The protein levels of collagen I and ALOX12 were measured in human lung tissues by Western blot. (B) Densitometry was used to analyze fold changes in the levels of ALOX12/α-actinin and collagen I /α-actinin in lung tissues of controls and IPF patients. * indicates $p < 0.05$ and *** indicates $p < 0.001$ compared with control.

TGF-β1 increases level of ALOX12 in human lung fibroblasts

Based on increased expression of ALOX12 in human lung tissue, we measured the level of ALOX12 in MRC-5 cells and primary human lung fibroblasts after TGF-β1 treatment to investigate the role of ALOX12 in the pathogenesis of pulmonary fibrosis. TGF-β1 increased the protein level of ALOX12, fibronectin, collagen I, and α-SMA in MRC-5 cells (Fig. 4A, B) and primary human lung fibroblasts (Fig. 4C, D). These results suggest that ALOX12 activity is associated with activation of fibroblasts by TGF-β1.

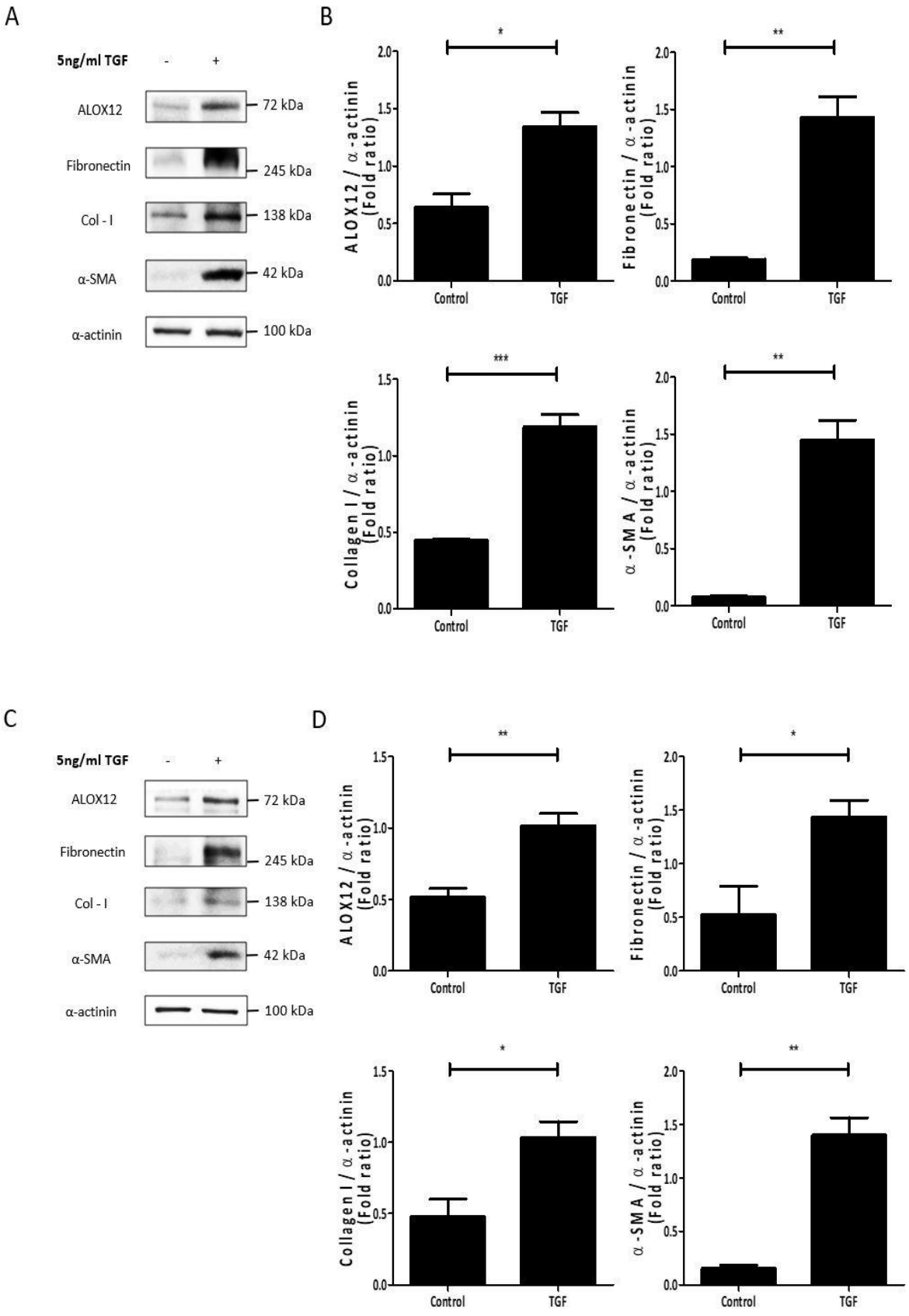
A
5ng/ml TGF - +
ALOX12
72 kDa
Fibronectin
245 kDa
Col - I
138 kDa
α-SMA
42 kDa
α-actinin
100 kDa
B
ALOX12 / α-actinin (Fold ratio)
Fibronectin / α-actinin (Fold ratio)
Collagen I / α-actinin (Fold ratio)
α-SMA / α-actinin (Fold ratio)
Control
TGF
C
5ng/ml TGF - +
ALOX12
72 kDa
Fibronectin
245 kDa
Col - I
138 kDa
α-SMA
42 kDa
α-actinin
100 kDa
D
ALOX12 / α-actinin (Fold ratio)
Fibronectin / α-actinin (Fold ratio)
Collagen I / α-actinin (Fold ratio)
α-SMA / α-actinin (Fold ratio)
Control
TGF

Figure 4. ALOX12 levels are increased in human lung fibroblasts treated with TGF- β1

(A) MRC-5 cells were treated with 5 ng/mL of TGF-β1 or vehicle for 24 hours. Total cells extracts were analyzed for protein levels of ALOX12, fibronectin, collagen I, and α-SMA by Western blotting. (B) Densitometry was used to analyses fold-changes in the levels of ALOX12/α-actinin, fibronectin/α-actinin, collagen I/α-actinin and α-SMA/α-actinin. * indicates $p < 0.05$, ** indicates $p < 0.01$, *** indicates $p < 0.001$ compared with control. (C) Primary human lung fibroblasts were treated with 5 ng/mL of TGF-β1 or vehicle for 24 hours. Total cells extracts were analyzed for protein levels of ALOX12, fibronectin, collagen I, and α-SMA by Western blotting. (D) Densitometry was used to analyses fold-changes in the levels of ALOX12/α-actinin and fibronectin/α-actinin, collagen I/α-actinin and α-SMA/α-actinin. * indicates $p < 0.05$, ** indicates $p < 0.01$ compared with control.

ALOX12 siRNA downregulates activation of fibroblasts treated with TGF- β1

To confirm that ALOX12 activity was essential for fibroblast activation, we investigated the effects of ALOX12 knockdown using specific siRNA. MRC-5 cells were transfected with control or ALOX12-specific siRNA, and then treated with TGF-β1 as indicated for 24 hours.

ALOX12-specific siRNA effectively downregulated the TGF-β1-induced expression of ALOX12 in MRC-5 cells (Fig. 5A, B), and primary human lung fibroblasts (Fig. 5C, D). ALOX12 knockdown also significantly inhibited the TGF-β1-induced expression of fibronectin, collagen type 1, and α-SMA (Fig. 5B, D).

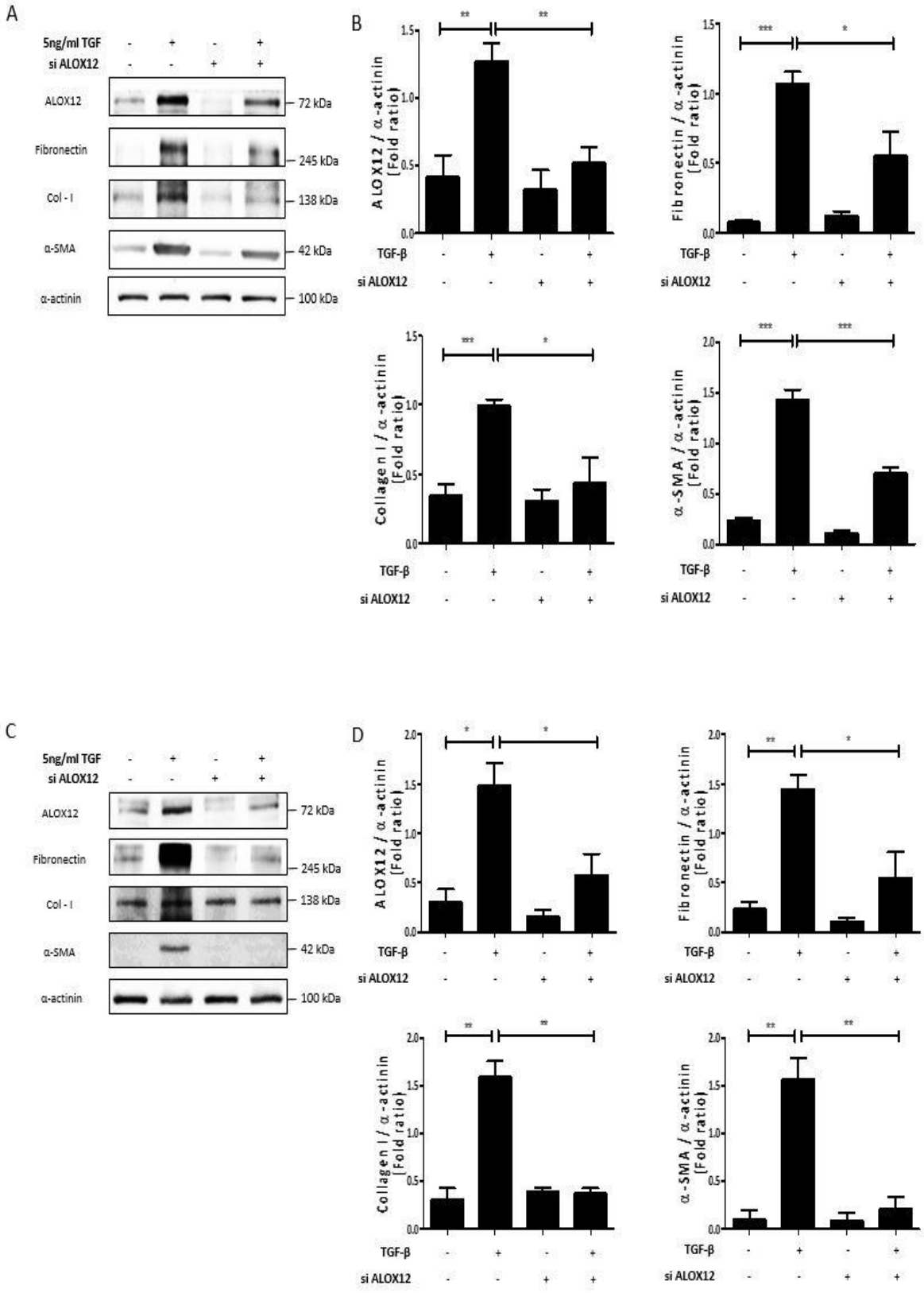
A
5ng/ml TGF
si ALOX12
ALOX12
Fibronectin
Col - I
α-SMA
α-actinin
72 kDa
245 kDa
138 kDa
42 kDa
100 kDa
B
ALOX12 / α-actinin (Fold ratio)
Fibronectin / α-actinin (Fold ratio)
Collagen I / α-actinin (Fold ratio)
α-SMA / α-actinin (Fold ratio)
TGF-β
si ALOX12
C
D

Figure 5. Inhibition of ALOX12 reduces TGF-β1 induced expression of fibrosis marker in fibroblasts

(A) MRC5 cells were treated with TGF-β1 for 24 hours after transfection with 30 pmol control siRNA or 30 pmol of ALOX12 specific siRNA for 48 hours. Upregulation of fibronectin, collagen I and α-SMA levels induced by TGF-β1 was inhibited by ALOX12 knockdown. (B) Densitometry was used to analyze fold changes in the levels of ALOX12/α-actinin, fibronectin/α-actinin, collagen I/α-actinin and α-SMA/α-actinin. * indicates $p < 0.05$, ** indicates $p < 0.01$ and *** indicates $p < 0.001$ compared with control. (C) Primary human lung fibroblasts were treated with TGF-β1 for 24 hours after transfection with 30 pmol control siRNA or 30 pmol of ALOX12 specific siRNA for 48 hours. Upregulation of fibronectin, collagen I and α-SMA levels induced by TGF-β1 was inhibited by ALOX12 knockdown. (D) Densitometry was used to analyze fold changes in the levels of ALOX12/α-actinin, fibronectin/α-actinin, collagen I/α-actinin and α-SMA/α-actinin. * indicates $p < 0.05$, ** indicates $p < 0.01$ and *** indicates $p < 0.001$ compared with control.

ALOX12 inhibitor suppresses activation of fibroblasts treated with TGF-β1

ML355, a selective inhibitor of ALOX12, has been known to have anti-thrombotic effects and protective effect against liver damage [28, 29]. TGF-β1 upregulated the expression of ALOX12, and ML355 effectively downregulated TGF-β1-induced expression of ALOX12 in a dose dependent manner in MRC-5 cell. ML355 also significantly inhibited the TGF-β1-induced expression of fibronectin and collagen type 1 (Fig. 6A, B). These results suggest that ALOX12 activity is essential for fibroblast activation.

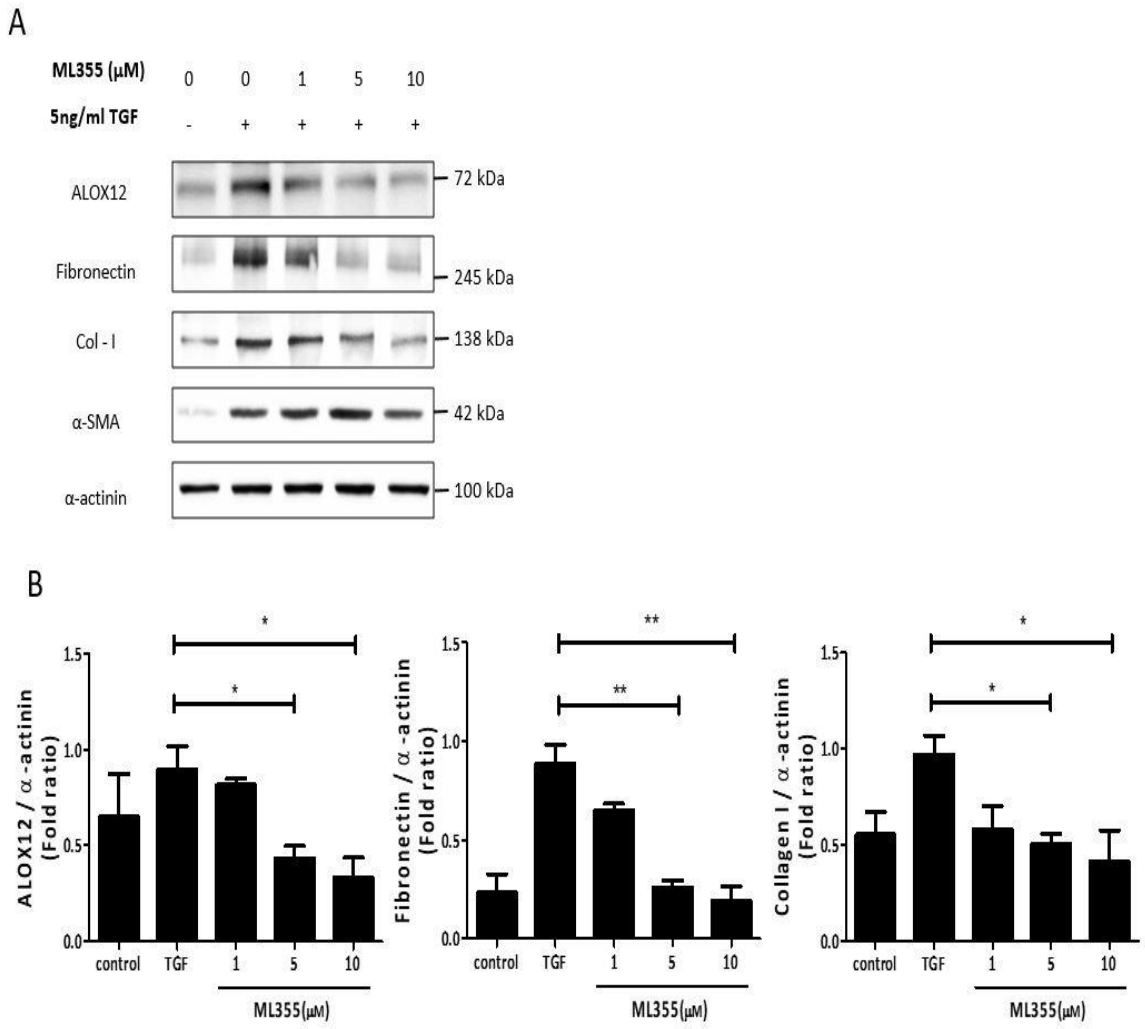

Figure 6. ML355 reduces TGF-β1 induced expression of fibrosis marker in fibroblasts

(A) MRC-5 cells were exposed to 5 ng/mL TGF-β1 simultaneously for 24 hours with ML355 (0, 1, 5, and 10 μM). Then, ALOX12, fibronectin, collagen I and α-SMA levels were measured by Western blot. ML355 decreased the protein levels of ALOX12 in MRC-5 cells in a dose-dependent manner. (B) Densitometry was used to analyze fold changes in the levels of ALOX12/α-actinin, fibronectin/α-actinin, collagen I/α-actinin. * indicates $p < 0.05$ and ** indicates $p < 0.01$ compared with control.

ALOX12 inhibitor suppresses TGF-β1-induced cell migration

We investigated whether ALOX12 inhibitor could suppress the migration of MRC-5 cells induced by TGF-β1. Cell migration was analyzed by wound healing assay. After scratching the cell culture dish at 0 hours, the drugs were treated, and photos were taken at 24 hours of scratch (Fig. 7A). Compared with vehicle, ML355 decreased the cell migration ratio up to ~ 0.42-fold, and TGF-β1 increased ~ 1.5-fold. However, compared with TGF treatment group, the ML355 + TGF-β1 treatment group reduced the cell migration rate by approximately ~2.6-fold (Fig. 7B).

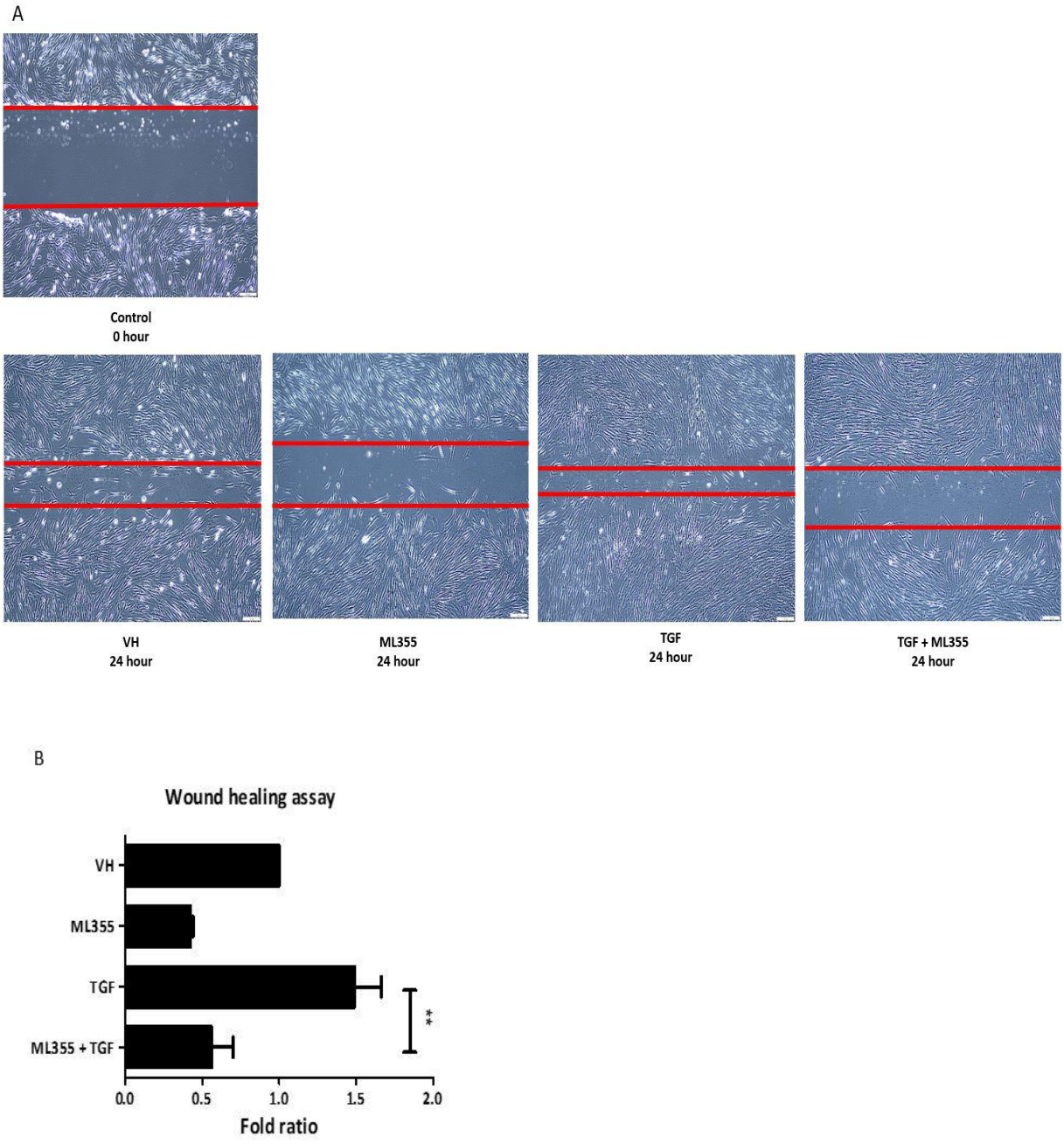

Figure 7. ML355 inhibits MRC-5 cell migration

Effect of ML355 on MRC-5 cell migration was examined by wound healing assay. (A) Images were from wound space of MRC-5 cells of 0 and 24 hours. (B) Densitometry was utilized to analyze the migrated fold-ratio. ** indicates $p < 0.01$ compared with TGF-β1; Mann-Whitney U test

ALOX12 inhibitor suppresses TGF-β1-induecd Smad signaling in fibroblasts

TGF-β1 stimulates the Smad signaling pathway, which is regulated via phosphorylation of Smad 2/3 [30]. TGF-β1 enhanced the phosphorylation of Smad 2/3 in MRC-5 cells, and ML355, ALOX12 inhibitor, suppressed these effects (Fig. 8A,B). These results suggest that ALOX12 inhibition has anti-fibrotic effects through suppression of TGF-β1-incuded Smad signaling pathway.

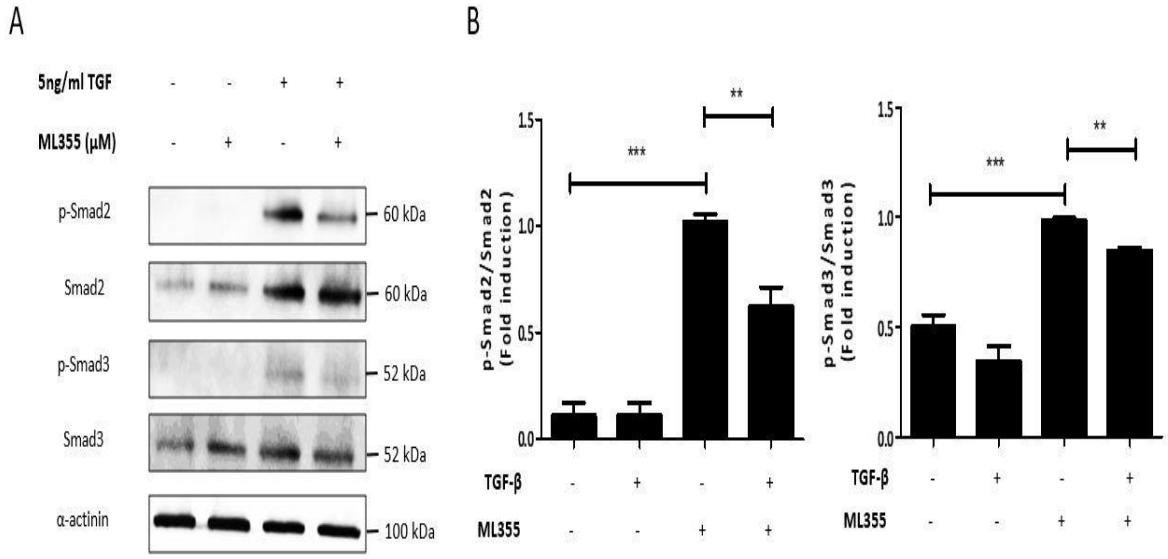

Figure 8. ML355 inhibits the TGF-β1-induced Smad signaling in MRC-5 cells

MRC-5 cells were pretreated with ML355 (10 μM) for 5 hours and then stimulated with 5 ng/mL of TGF-β1 for 1 hour. (A) Total cell extracts were analyzed for protein levels of p-Smad 2/3, and Smad 2/3 by Western blotting. (B) Densitometry was used to analyze for fold changes in the levels of p-Smad2/Smad2 and p-Smad3/Smad3. The mean values from three independent experiments are shown in the graphs. ** indicates $p < 0.01$, *** indicates $p < 0.001$.

ALOX12 inhibitor attenuates bleomycin-induced pulmonary fibrosis in mice

We used bleomycin-induced pulmonary fibrosis mouse model to determine the anti-fibrotic effect of ML355 in *in vivo* models. ML355 was administered by oral gavage at a dose of 15 mg/kg every 2 days for 2 weeks from 7 days after bleomycin treatment. Then, the mice were sacrificed, and the lungs were harvested on 21 days. Bleomycin-induced mice showed higher weight loss after bleomycin administration compared to that of the control mice, but ML355 significantly attenuated the bleomycin-induced weight loss (Fig. 9A). The intensity of lung fibrosis in the bleomycin plus ML355 group was less than bleomycin-treated group (Fig. 9B). The Ashcroft score of the bleomycin plus ML355 group was numerically lower than the bleomycin group (Fig. 9C). Mice treated with bleomycin showed much higher levels of hydroxyproline than control but ML355 significantly reduced them (Fig. 9D). Our results suggest that inhibition of ALOX12 may have therapeutic effects in pulmonary fibrosis.

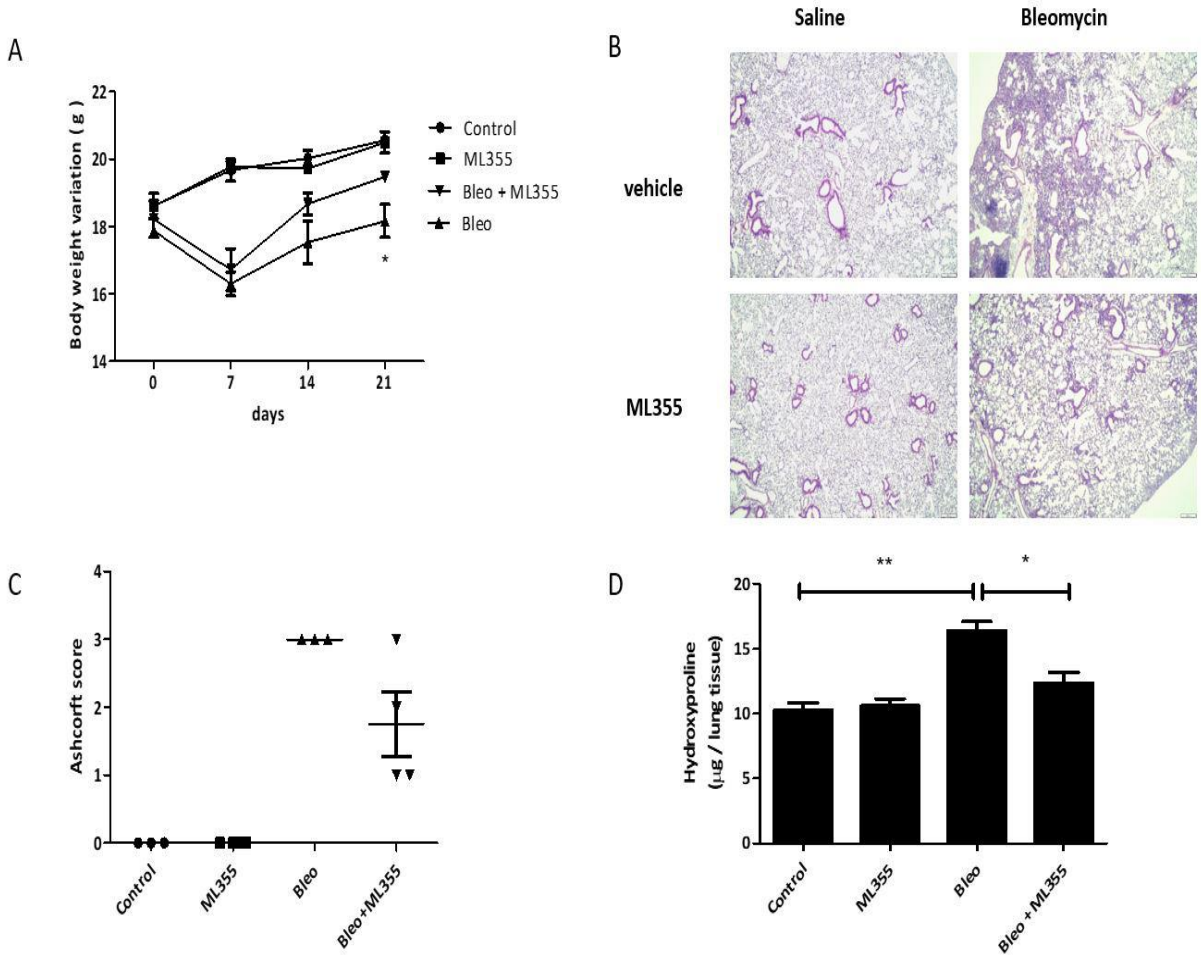

Figure 9. Attenuation of bleomycin-induced pulmonary fibrosis by ALOX12 inhibitor

(A) ML355 (15 mg/kg) was administered to mice 3 days/week for 2 weeks after 7 days intratracheal injection of bleomycin (3 U/kg). Body weights were analyzed for four groups of mice: control (n=3), ML355 treatment (n=4), bleomycin treatment (n=3) and bleomycin plus ML355 (n=4). * indicates $p < 0.05$ compared with control. (B) Representative histologic lung sections from each group stained with hematoxylin and eosin. (C) Lung fibrosis was measured by Ashcroft score. (D) Collagen content was estimated by hydroxyproline assay. * indicates $p < 0.05$ and ** indicates $p < 0.01$; unpaired t-test.

Discussion

In this study, through metabolic profiling, the alteration of eicosanoid metabolites was observed in plasma of patients with IPF compared with controls. We also showed that 12(S)-HETE promotes activation of human lung fibroblasts. Arachidonic acid-derived metabolite, 12(S)-HETE is catalyzed by ALOX12 [18], and the protein level of ALOX12 increased in fibroblasts after TGF-β1 stimulation. We presented the association between fibroblasts and ALOX12 activation through inhibition of TGF-β1-induced activation of fibroblasts by ALOX12 specific siRNA. Also, ALOX12 inhibitor inhibited TGF-β1 induced fibrosis marker such as fibronectin and collagen I in fibroblasts. *In vivo* study, ALOX12 inhibitors also alleviate bleomycin-induced pulmonary fibrosis in mice. Our results suggest that ALOX12 is associated with pathogenesis of IPF, and is implicated as a potential therapeutic target in IPF.

Metabolic profiling can identifies disease-related substances and characterize metabolic changes in the pathogenesis of IPF [31]. Lipid metabolites remodel cell membrane structures, energy storage and transmitting signals *in vivo* and *in vitro*, among which lysophospholipids, sphingolipids, and eicosanoids are known to be involved in the process of fibrosis [32]. Since alterations in metabolic pathways for energy consumption contribute to IPF pathogenesis, metabolites may contribute to predict diagnosis and prognosis of IPF [11]. We performed metabolic profiling in human plasma, and then I focused on 12(S)-HETE. Our results showed that 12(S)-HETE levels were significantly higher in IPF patients. In addition, level of plasma 12(S)-HETE of systemic sclerosis (SSc) was significantly higher than control group [33].

ALOX12 is also involved in regulating cancer metastasis by metabolizing

arachidonic acid to 12(S)-HETE [34]. In a previous study, the depletion of ALOX12 alone had the effect of inhibiting the growth of breast cancer cells and inducing apoptosis and ALOX12 mediates early inflammation in bone recovery, ML355, ALOX12 inhibitor, inhibited the production of ALOX12, and affected the expression of anti-inflammatory cytokines/proteins [35, 36]. Our data showed that TGF-β1 increases level of ALOX12 in human lung fibroblasts, and when we inhibit ALOX12 by treatment with ML355 or ALOX12 siRNA, we found that the expression fibrosis marker decreased, suggesting the role of ALOX12 in pulmonary fibrosis. These results suggested that ALOX12 is associated with activation of fibroblasts, and ALOX12 inhibition may have the effect of advanced anti-inflammatory agents, but it may have an anti-fibrotic effect through our experiments.

Since ALOX12 is known to function of cell migration in previous studies [18], we examined the cell migration ratio by wound healing assay in MRC-5 cells. When the ALOX12 inhibitor treated with TGF-β1, cell migration was inhibited significantly compared with TGF-β1. These results suggest that ALOX12 inhibitor have not only anti-fibrotic effect on protein expression, but also the inhibitory ability of fibroblast migration.

TGF-β1 is regulated by intracellular signaling via Smad molecules [37]. TGF-β isoforms induce intracellular signaling through Smad 2/3 transcription factors [38]. According to our study, we found that ALOX12 inhibitor reduced TGF-β1 induced phosphorylation of Smad 2/3 in human lung fibroblasts. Thus, our results suggest that inhibition of ALOX12 might have an anti-fibrotic effect via inhibition of TGF-β1- Smad signaling pathway.

ML355 is known as an antiplatelet drug for inhibition of thrombosis in mice [28]. It has not been known whether ML355 plays in the pulmonary fibrosis mechanism. As our data confirmed that fibroblasts are associated with ALOX12, we tested the anti-fibrotic effects of

ML355 in *in vivo* models using bleomycin-induced pulmonary fibrosis mice as ALOX12 inhibitor. ML355 preserved weight reduced by bleomycin injection, and hydroxyproline levels were also reduced.

Conclusions

Our results suggest that ALOX12 might be associated with the pathogenesis of pulmonary fibrosis, and is implicated as a potential therapeutic target in IPF.

References

1. Richeldi, L., H.R. Collard, and M.G. Jones, *Idiopathic pulmonary fibrosis.* The Lancet, 2017. **389**(10082): p. 1941-1952.
2. Hoo, Z.H. and M.K. Whyte, *Idiopathic pulmonary fibrosis.* Thorax, 2012. **67**(8): p. 742-746.
3. Coward, W.R., G. Saini, and G. Jenkins, *The pathogenesis of idiopathic pulmonary fibrosis.* Therapeutic advances in respiratory disease, 2010. **4**(6): p. 367-388.
4. Liu, R.-M. and K.G. Pravia, *Oxidative stress and glutathione in TGF-β-mediated fibrogenesis.* Free Radical Biology and Medicine, 2010. **48**(1): p. 1-15.
5. Selman, M., T.E. King Jr, and A. Pardo, *Idiopathic pulmonary fibrosis: prevailing and evolving hypotheses about its pathogenesis and implications for therapy.* Annals of internal medicine, 2001. **134**(2): p. 136-151.
6. Maher, T., A. Wells, and G. Laurent, *Idiopathic pulmonary fibrosis: multiple causes and multiple mechanisms?* European Respiratory Journal, 2007. **30**(5): p. 835-839.
7. Sgalla, G., et al., *Idiopathic pulmonary fibrosis: pathogenesis and management.* Respiratory research, 2018. **19**(1): p. 1-18.
8. Richeldi, L., et al., *Efficacy and safety of nintedanib in patients with advanced idiopathic pulmonary fibrosis.* BMC pulmonary medicine, 2020. **20**(1): p. 1-8.
9. Vietri, L., et al., *Pirfenidone in idiopathic pulmonary fibrosis: real-life experience in the referral centre of Siena.* Therapeutic advances in respiratory disease, 2020. **14**: p. 1753466620906326.
10. Suryadevara, V., et al., *Lipid mediators regulate pulmonary fibrosis: potential mechanisms and signaling pathways.* International journal of molecular sciences, 2020. **21**(12): p. 4257.

11. Zhao, Y.D., et al., *Metabolic heterogeneity of idiopathic pulmonary fibrosis: a metabolomic study.* BMJ open respiratory research, 2017. **4**(1): p. e000183.

12. Wang, B., et al., *Metabolism pathways of arachidonic acids: mechanisms and potential therapeutic targets.* Signal transduction and targeted therapy, 2021. **6**(1): p. 1-30.

13. Capra, V., et al., *Eicosanoids and their drugs in cardiovascular diseases: focus on atherosclerosis and stroke.* Medicinal research reviews, 2013. **33**(2): p. 364-438.

14. Sonnweber, T., et al., *Arachidonic acid metabolites in cardiovascular and metabolic diseases.* International journal of molecular sciences, 2018. **19**(11): p. 3285.

15. Sarsour, E.H., et al., *Arachidonate 12-lipoxygenase and 12-hydroxyeicosatetraenoic acid contribute to stromal aging-induced progression of pancreatic cancer.* Journal of Biological Chemistry, 2020. **295**(20): p. 6946-6957.

16. Gotoh, Y., et al., *Lipid peroxide-induced redox imbalance differentially mediates CaCo-2 cell proliferation and growth arrest.* Cell proliferation, 2002. **35**(4): p. 221-235.

17. Wang, H.P., et al., *Phospholipid hydroperoxide glutathione peroxidase induces a delay in G1 of the cell cycle.* Free radical research, 2003. **37**(6): p. 621-630.

18. Zheng, Z., et al., *The biological role of arachidonic acid 12-lipoxygenase (ALOX12) in various human diseases.* Biomedicine & Pharmacotherapy, 2020. **129**: p. 110354.

19. Weaver, J.R., et al., *Integration of pro-inflammatory cytokines, 12-lipoxygenase and NOX-1 in pancreatic islet beta cell dysfunction.* Molecular and cellular endocrinology, 2012. **358**(1): p. 88-95.

20. Tahmasbpour, E., et al., *Altered expression of cyclooxygenase-2, 12-lipoxygenase, inducible nitric oxide synthase-2 and surfactant protein D in lungs of patients with pulmonary injury caused by sulfur mustard.* Drug and chemical toxicology, 2019. **42**(3): p. 257-263.

21. Mishra, B.B., et al., *Nitric oxide prevents a pathogen-permissive granulocytic inflammation during tuberculosis.* Nature microbiology, 2017. **2**(7): p. 1-11.

22. Chung, E.J., et al., *12-lipoxygenase is a critical mediator of type II pneumocyte senescence, macrophage polarization and pulmonary fibrosis after irradiation.* Radiation research, 2019. **192**(4): p. 367-379.

23. Chiaramonte, M.G., et al., *IL-13 is a key regulatory cytokine for Th2 cell-mediated pulmonary granuloma formation and IgE responses induced by Schistosoma mansoni eggs.* The Journal of Immunology, 1999. **162**(2): p. 920-930.

24. Zhu, Z., et al., *Pulmonary expression of interleukin-13 causes inflammation, mucus hypersecretion, subepithelial fibrosis, physiologic abnormalities, and eotaxin production.* The Journal of clinical investigation, 1999. **103**(6): p. 779-788.

25. Raghu, G., et al., *An official ATS/ERS/JRS/ALAT statement: idiopathic pulmonary fibrosis: evidence-based guidelines for diagnosis and management.* American journal of respiratory and critical care medicine, 2011. **183**(6): p. 788-824.

26. Yang, J., et al., *Quantitative profiling method for oxylipin metabolome by liquid chromatography electrospray ionization tandem mass spectrometry.* Analytical chemistry, 2009. **81**(19): p. 8085-8093.

27. Ashcroft, T., J.M. Simpson, and V. Timbrell, *Simple method of estimating severity of pulmonary fibrosis on a numerical scale.* Journal of clinical pathology, 1988. **41**(4): p. 467-470.

28. Adili, R., et al., *First selective 12-LOX inhibitor, ML355, impairs thrombus formation and vessel occlusion in vivo with minimal effects on hemostasis.* Arteriosclerosis, thrombosis, and vascular biology, 2017. **37**(10): p. 1828-1839.

29. Zhang, X.-J., et al., *An ALOX12–12-HETE–GPR31 signaling axis is a key mediator of*

hepatic ischemia–reperfusion injury. Nature medicine, 2018. **24**(1): p. 73-83.

30. Chitra, P., et al., *Berberine inhibits Smad and non-Smad signaling cascades and enhances autophagy against pulmonary fibrosis.* Journal of molecular medicine, 2015. **93**(9): p. 1015-1031.

31. Kang, Y.P., et al., *Metabolic profiling regarding pathogenesis of idiopathic pulmonary fibrosis.* Journal of proteome research, 2016. **15**(5): p. 1717-1724.

32. Castelino, F.V., *Lipids and eicosanoids in fibrosis: emerging targets for therapy.* Current opinion in rheumatology, 2012. **24**(6): p. 649-655.

33. González-Núñez, D., et al., *Increased levels of 12 (S)-HETE in patients with essential hypertension.* Hypertension, 2001. **37**(2): p. 334-338.

34. Contursi, A., et al., *Platelets induce free and phospholipid-esterified 12-hydroxyeicosatetraenoic acid generation in colon cancer cells by delivering 12-lipoxygenase.* Journal of lipid research, 2021. **62**.

35. Huang, Z., et al., *ALOX12 inhibition sensitizes breast cancer to chemotherapy via AMPK activation and inhibition of lipid synthesis.* Biochemical and biophysical research communications, 2019. **514**(1): p. 24-30.

36. Yao, D., et al., *Matrix stiffness regulates bone repair by modulating 12-lipoxygenase-mediated early inflammation.* Materials Science and Engineering: C, 2021. **128**: p. 112359.

37. Tzavlaki, K. and A. Moustakas, *TGF-β Signaling.* Biomolecules, 2020. **10**(3): p. 487.

38. Walton, K.L., K.E. Johnson, and C.A. Harrison, *Targeting TGF-β mediated SMAD signaling for the prevention of fibrosis.* Frontiers in pharmacology, 2017. **8**: p. 461.

국 문 요 약

연구 배경: 특발성 폐섬유증(idiopathic pulmonary fibrosis, IPF)은 간질성 폐질환의 한 종류로, 현재까지 원인이 정확히 알려져 있지 않고 만성적으로 진행하는 질환이다. 예후는 매우 불량하여 환자는 진단 후 3-4년 내 호흡부전 등으로 사망하게 된다. 특발성 폐섬유증 발병에 있어서 대사체의 역할은 아직 잘 알려지지 않다. 12(S)-hydroxyeicosatetraenoic acid (12(S)-HETE)는 사람 혈소판 또는 백혈구에서 arachidonic acid 12-lipoxygenase (ALOX12)의 효소를 통해 생성되는 arachidonic acid 대사체이다. 본 연구에서는 특발성폐섬유증에서 12(S)-HETE와 ALOX12의 역할을 확인하고자 하였다.

실험 방법: IPF 환자 76명과 정상 대조군 40명의 혈장에서 LC-MS/MS를 이용하여 12(S)-HETE 농도를 측정하였다. IPF 환자 6명과 정상 대조군 6명의 폐 조직을 이용하여 ALOX12 농도를 측정하였다. 12(S)-HETE와 ALOX12의 기능은 ALOX12 억제제 또는 siRNA를 사용하여 TGF-β1를 처리한 인간 유래 폐 섬유아세포에서 확인하였다. ALOX12 억제제의 항섬유화 효과는 섬유화 마커변화와 migration assay를 통해 확인하였다. 또한, 폐 섬유화 동물 모델인 블레오마이신 폐 손상 마우스에 ALOX12 억제제를 경구 투여하여 확인하였다.

결과: IPF 환자군에서 혈액내 12(S)-HETE 농도가 정상 대조군 보다 유의적으로 증가하였고, 12(S)-HETE는 인간 유래 폐 섬유아세포에서의 collagen I 과 fibronectin의 단백질 발현을 증가시켰다. ALOX12의 농도는 IPF 환자군에서 ALOX12 농도는 정상 대조군 보다 유의적으로 증가되어 있는 것을 확인하였다. 또한, IPF 환자의 폐 조직과 TGF-β1에 의해 자극된 인간 유래 폐 섬유아세포에서도 확인해본 결과, ALOX12의 농도가 대조군 보다 증가하였다. ALOX의 억제제 및 ALOX12 특이적 siRNA는 인간 유래 폐 섬유아

세포에서 TGF-β1 자극에 의해 증가한 collagen I 과 fibronectin의 발현을 감소시켰다. ALOX12 억제제는 인간 유래 폐 섬유아세포의 세포 이동을 억제하고 TGF-β1에 의한 Smad2/3의 인산화를 억제하였다. 폐 섬유화 동물 모델인 블레오마이신을 기도내 처리한 마우스에서 ALOX12의 억제제는 hydroxyproline 농도를 감소시켰다.

결론: 본 연구는 ALOX12 가 IPF의 병태 생리와 관련이 있고, 그 억제제가 TGF-β1-Smad 신호 전달 경로의 차단을 통해 항 섬유화 효과를 보일 수 있음을 확인하여, ALOX12의 특발성 폐섬유증의 잠재적 치료 대상으로서의 가능성을 제시하였다.